






## MINIREVIEW

[View Article Online](#)  
[View Journal](#) | [View Issue](#)
Cite this: *Nanoscale*, 2025, **17**, 17004

# Advances in carbon nanomembranes for separation: from free-standing films to composite structures

 Ana Ambrož, <sup>a,b</sup> Albert Schnieders, <sup>c</sup> Claus Hélix-Nielsen, <sup>a,d</sup>  
 Armin Götzhäuser <sup>\*b</sup> and Irena Petrinic <sup>a</sup>

This work reviews the development and application potential of carbon nanomembranes (CNMs) especially for separation purposes, starting from self-assembled monolayers (SAMs) as a representative pre-stage of CNMs to their evolution into composite membranes. SAMs form spontaneously on surfaces through intrinsic chemical functionalities, providing the basis for advanced 2-dimensional materials. The transition from SAMs to CNMs involves electron irradiation-induced crosslinking, producing robust, free-standing molecular thin sheets with high resistance to wet etching and customizable functionalities. To enhance mechanical robustness, ease of handling, and scalability, CNM-composite membranes are fabricated by combining CNMs directly with porous support materials like track-etched polyethylene terephthalate (TE-PET) paving the way for future industrial applications.

Received 20th December 2024,

Accepted 6th June 2025

DOI: 10.1039/d4nr05361c

[rsc.li/nanoscale](https://rsc.li/nanoscale)

<sup>a</sup>University of Maribor, Faculty of Chemistry and Chemical Engineering, Smetanova ulica 17, 2000 Maribor, Slovenia

<sup>b</sup>University of Bielefeld, Faculty of Physics, Universitätsstrasse 25, 33615 Bielefeld, Germany. E-mail: [goetzhaeuser@physik.uni-bielefeld.de](mailto:goetzhaeuser@physik.uni-bielefeld.de)

<sup>c</sup>CNM Technologies GmbH, Blomestr. 10, 33609 Bielefeld, Germany

<sup>d</sup>Technical University of Denmark, Department of Environmental and Resource Engineering, Brovej 118, 2800 Kgs., Lyngby, Denmark

## 1. Introduction

Self-assembled monolayers (SAMs) have drawn significant interest over the past decades due to their ability to form spontaneously through the self-organization of molecules on a substrate. This process allows for the creation of well-ordered, functional molecular-thin films providing the basis for advanced 2-dimensional materials. Carbon nanomembranes (CNMs) are fabricated from SAMs and other thin assemblies of



Ana Ambrož

Ana Ambrož earned her MSc degree in Chemical Engineering in 2021 from the Faculty of Chemistry and Chemical Engineering, University of Maribor, Slovenia. She is currently in the final year of her PhD in Chemical Engineering, focusing on the development of carbon nanomembranes as innovative solutions to key challenges in filtration technologies.



Albert Schnieders

Dr Albert Schnieders is co-founder and CEO of CNM Technologies, which produces molecular thin, carbon nanomembranes (CNMs) and develops innovative applications of CNMs in a diverse field of industries. Focus technologies is water filtration. Albert earned his degree in physics at the University of Münster, Germany. After working as a postdoctoral researcher at the Universities of Utah and Delaware, he worked for the US subsidiaries of two German companies: Tascon, a contract laboratory specializing in chemical surface analysis, and the scientific instrument manufacturer ION-TOF. Albert left both companies and the USA end of 2011 to start CNM Technologies.



molecular precursors through electron irradiation, converting them into molecular sheets, which are robust enough to be even handled free-standing. This transformation enhances the material's mechanical strength and etching resistance in wet conditions while enabling precise tuning of properties like crosslinking density, thickness, chemical stability, permeability, and selectivity. With their high surface-to-volume ratio and remarkable stability, CNMs hold promise for a variety of applications, ranging from filtration technologies<sup>1–3</sup> to electronic devices.<sup>4–6</sup> However, the practical use of CNMs often requires their integration with porous support materials to maintain their mechanical stability and functionality. Among various support material options for separation purposes, track-etched (TE) membranes are particularly attractive due to their precisely controlled pore structures and strong mechanical properties. To overcome the challenges and risks of ruptures and defects during substrate-to-support transfer, CNM-composite membranes have been developed. In these membranes, the CNM is directly fabricated onto the porous support material, removing the need for a transfer step and thus minimizing the risk of damage and performance degradation. This paper offers an overview of the evolution from SAMs to CNMs, including fabrication methods, properties, and their applications in separation technologies. It also examines the potential of CNMs across different fields and the role of support materials in optimizing their performance.

## 2. SAMs

Self-assembly is a process in which disordered elements spontaneously organize into a cohesive structure through localized interactions among the elements. As the name implies, without the need for external guidance, this natural phenomenon

enables nanostructures to form autonomously.<sup>7</sup> It commences with the assembly of individual building blocks, each possessing intrinsic properties indirectly encoding the blueprint of the final structure. As the self-assembly progresses, the components interact, ultimately culminating in the formation of a complete structure.<sup>7</sup> This spontaneous organization emerges through the interplay of forces acting across different scales, organizing different types of matter, such as atoms, molecules, colloids, and polymers into more complex structures.<sup>8</sup> Molecules or ligands constituting SAMs possess a chemical functionality, often referred to as a 'headgroup', which exhibits a particular affinity for a substrate.<sup>9–11</sup> The structure of SAMs is therefore fundamentally influenced by the interaction between headgroup/substrate and intermolecular interactions.<sup>12</sup> The self-assembly process enables the creation of well-ordered monolayers with tailored properties, allowing precise control over surface wettability,<sup>13</sup> chemical reactivity,<sup>14</sup> electronic behaviour,<sup>15</sup> and biocompatibility.<sup>13</sup> Such tuneable characteristics have been effectively leveraged for applications in surface functionalization and molecular sensing.<sup>16</sup>

The advancements in SAMs are grounded in the pioneering work of Langmuir and Blodgett, whose studies in 1935 laid the foundation for monolayer self-assembly.<sup>17–19</sup> Langmuir observed that molecularly thin films formed at the water–air interface consist of amphiphilic molecules oriented at the water surface, with their polar functional groups interacting with the aqueous phase and their nonpolar moieties extending into the air phase.<sup>17,18</sup> These experiments provided strong evidence for the presence of short-range forces and offered an explanation for why certain molecules formed stable monolayer films while others did not.<sup>17</sup> Langmuir's findings were further advanced by Blodgett, who developed a method to transfer these monolayer films from the water surface onto solid substrates, resulting in what are now known as



**Claus Hélix-Nielsen**

*Claus Hélix-Nielsen holds a PhD in Chemical Engineering from the Technical University of Denmark (DTU) where he is currently professor and Head of Department of Environmental and Resource Engineering. His research primarily focuses on process systems engineering, optimization, and the development of sustainable energy systems. He has received multiple awards for his significant contributions to the field, including the European Inventor award 2014 in the category: small and medium-sized enterprises (SMEs) for patent WO 2006/122566 from the European Patent Office.*

ing the European Inventor award 2014 in the category: small and medium-sized enterprises (SMEs) for patent WO 2006/122566 from the European Patent Office.



**Armin Götzhäuser**

*Prof. Dr Armin Götzhäuser earned his PhD in Physical Chemistry from the University of Heidelberg in 1993. After completing his postdoctoral research at the University of Illinois at Urbana-Champaign, he held academic positions at the University of Heidelberg, University of Marburg, and Bielefeld University, where he is currently a professor of Experimental Physics. He is also the founder of the Bielefeld Institute for*

*Biophysics and Nanoscience (BINAS) and has been involved in various international research initiatives. His research focuses on supramolecular systems, surfaces, and nanoscience, with a particular emphasis on innovative applications of carbon nanomembranes.*



Langmuir–Blodgett (LB) films.<sup>17</sup> In 1946, Bigelow and others observed that long-chain alkylamines form a densely packed layer on the surface of platinum.<sup>8,20</sup> In 1978 Sagiv prepared alkylsilane monolayers on silicon surfaces, which can be considered as the first SAMs.<sup>21,22</sup> In 1983, another significant breakthrough was made by Nuzzo and Allara when they conducted experiments involving gold surfaces and alkyl disulfides. Through their work, they discovered that the alkyl disulfides formed tightly packed monolayers of chemisorbed alkanedithiolate molecules on the gold surface.<sup>23</sup> This finding opened new possibilities for studying and manipulating molecular layers on solid surfaces, with potential applications ranging from nanotechnology to biosensors.<sup>9</sup> The high affinity of thiols for surfaces of noble metals allows for the formation of well-defined organic surfaces, where specific chemical functionalities, derived from the molecules or ligands that constitute SAMs, are displayed at the exposed interface, providing versatility and utility in various applications.<sup>10,11,24,25</sup> Following the immersion of a gold surface into a thiol solution, the S–H bond of the thiol dissociates, releasing hydrogen and forming covalent Au–S bonds.<sup>10,26</sup> Subsequently, intermolecular interactions induce lateral ordering of the molecular backbones, leading to the formation of well-ordered monolayers.<sup>25,27</sup> This organization is a result of the strong interactions between the metal atoms and sulfur atoms present in the thiol molecules. These metal–sulfur interactions not only contribute to the stability of the SAMs but also allow them to maintain their integrity in different environments.<sup>10</sup> In addition to thiols, other classes of molecules, such as phosphonic acids,<sup>28–30</sup> silanes,<sup>31,32</sup> and carboxylates,<sup>33–36</sup> are also commonly used in the formation of SAMs. These molecules interact with various substrates through different bonding mechanisms, such as covalent bonding or electrostatic interactions, allowing for a broad range of functionalized surfaces. To obtain SAMs with a desired molecular packing, parameters

like immersion time, temperature, concentration, and polarity of the solvents as well as the molecular species itself can be adjusted.<sup>37</sup>

### 3. From SAMs to CNMs

Surface-bound aromatic SAMs can be converted into free-standing CNMs *via* crosslinking induced by electron irradiation. After crosslinking, they can be released from the substrate by selective cleavage of the anchor group–substrate bond<sup>1,38</sup> or by the dissolution of the substrate<sup>39,40</sup> and transferred onto new solid or perforated supports material (*e.g.*, grids)<sup>41</sup> as free-standing, molecular thin nanosheets (Fig. 1).<sup>42</sup> The process of transferring CNM from the original substrate to a different solid support or perforated structure, such as a transmission electron microscopy (TEM) grid, usually begins with the application of a polymeric transfer medium (acting as a stabilizing layer) to the CNM and dissolving the original substrate. The hardened stabilizing layer with the attached CNM is transferred onto another solid support material. Finally, the stabilizing layer is dissolved, leaving the CNM adhered to the new support material.<sup>41,43</sup>

The initial requirement for transforming SAMs into nanomembranes is a durable framework that can withstand electron irradiation and facilitate the formation of intermolecular crosslinks. Additionally, they must exhibit a substantial density of carbon atoms, which is typically met by SAMs containing a significant proportion of aromatic groups.<sup>37</sup> The crosslinking of molecules in SAMs has been demonstrated to take place with various polyaromatic thiols.<sup>37</sup> In addition to thiols, CNMs with carboxylic anchoring groups were successfully formed on silver substrates,<sup>33–36</sup> presenting new possibilities for filtration applications.<sup>33</sup> Exploring further alternatives to sulfur-based monolayers, N-heterocyclic carbenes (NHCs) based SAMs on gold, where the carbene carbon atom serves as the anchoring group, have been explored in recent years.<sup>45–48</sup> These monolayers have shown exceptional chemical, electrochemical, and thermal stability, attributed to the stronger gold–carbon bond compared to the weaker gold–sulfur bond.<sup>45,46</sup>

The synthesis of CNMs through electron-induced methods has conventionally been conducted on gold<sup>49</sup> and silver substrates,<sup>33</sup> on silicon nitride surfaces,<sup>42</sup> and on aluminium substrates.<sup>50</sup> Under electron irradiation carbon–hydrogen bonds are cleaved, followed by the formation of carbon–carbon crosslinks between the aromatic units (Fig. 2).<sup>42</sup> The specific crosslinking mechanisms are strongly influenced by the electron energy.<sup>45,51</sup> Neumann *et al.* studied the effect of different electron energies ranging from 2.5 to 100 eV, on the crosslinking of 4'-nitro-1,1'-biphenyl-4-thiol (NBPT) SAM on gold.<sup>51</sup> The results show a strong correlation between the electron energy and the required electron dose for fully crosslinking an NBPT SAM on gold into a CNM. Two mechanisms of C–H bond scission have been identified, leading to crosslinking at high and low electron energies. At high electron energies (6.5–100 eV), crosslinking is primarily



**Irena Petrić**

*Irena Petrić received her PhD in 2006 from the Faculty of Mechanical Engineering, University of Maribor, Slovenia. She is currently an Associate Professor in Chemical Engineering at the Faculty of Chemistry and Chemical Engineering, University of Maribor and in the Faculty of Environmental Protection, Velenje, Slovenia. Her research focuses on aqueous resource recovery using membrane technology, particularly forward osmosis. She contributed to the establishment of the Laboratory for Water Biophysics and Membrane Processes and has led several industrial projects on membrane applications and characterization.*



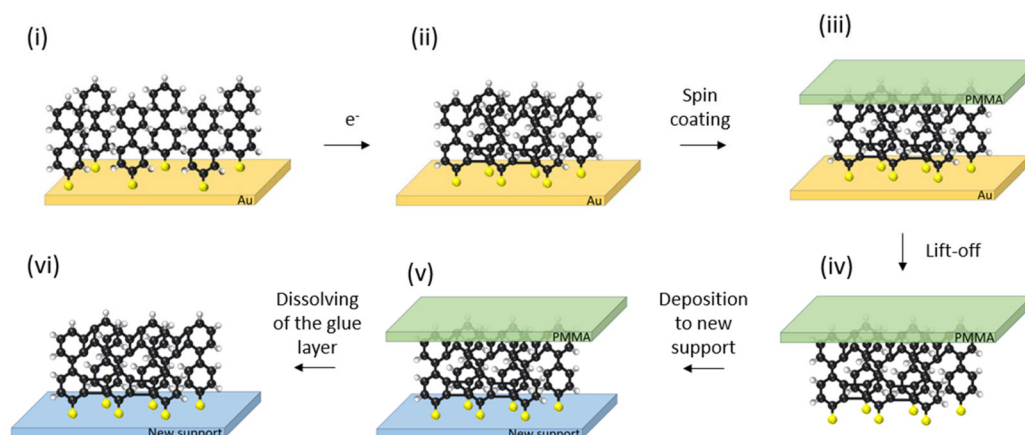


**Fig. 1** Schematics of the structure and fabrication of a CNM (adapted from ref. 44). The fabrication process involves (i) molecular self-assembly on a solid surface (e.g. Au), (ii) radiation-induced 2D polymerization and (iii) application of a transfer medium-(iv) lift-off of the network of crosslinked molecules supported by the transfer medium, (v) transfer to the new support material, (vi) dissolving of the transfer medium to obtain CNM on new support material.<sup>41</sup>

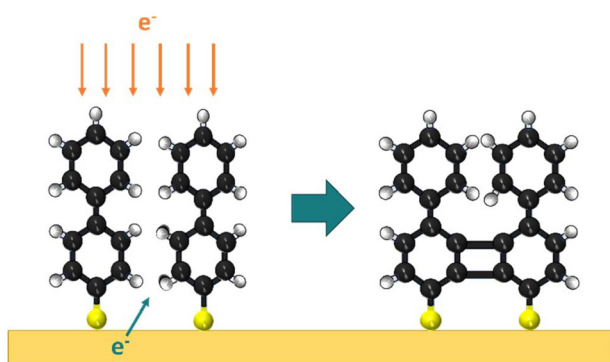


**Fig. 2** Schematic presentation of crosslinking of biphenylthiol-based monolayers with electron irradiation.<sup>56</sup>

surface-active and end-group characteristics of the molecular precursors. A monomolecular SAM transforms to a CNM with consistent surface chemical groups, while a mixed molecular SAM of molecules with different chemical end groups can result in a CNM with varied surface functionalities. The cross-linked SAMs exhibit a high etching resistance,<sup>52</sup> block electrochemical deposition,<sup>53</sup> and can be chemically functionalized.<sup>54</sup> Consequently, smart molecular design can tailor the chemical functionalities on both faces of the membrane.<sup>44</sup> It has been shown that optimizing molecular design can significantly influence membrane performance, enabling the development of membranes with customized properties, such as permeation rate, solute selectivity, adsorption enthalpy, mechanical strength, and chemical resistance.<sup>35,44,55</sup>

driven by direct electron impact ionization, whereas at low electron energies (2.5–6.5 eV), dissociative electron attachment is the dominant process. Furthermore, Cegiela *et al.* explored the impact of electron irradiation on N-heterocyclic carbenes (NHCs) with varying benzene moieties and nitrogen side group sizes to refine their structural properties. Their findings establish key design strategies for optimizing NHC SAMs, enabling efficient electron-beam modification and the fabrication of sulfur-free CNMs. Notably, NHC monolayers exhibit significantly greater stability in their bonding with metal substrates under electron irradiation compared to conventional thiols or carboxylic acids.<sup>45</sup>

Carbon nanomembranes inherit structural and functional elements from their parenting SAMs.<sup>49</sup> By varying the type of precursor molecules, the thickness of the aromatic monolayers can be controlled, which opens new avenues for the engineering of nanomembranes.<sup>37,49</sup> The packing density and lateral organization within the parent SAM dictate both the mass density and the porosity of the resultant CNM.<sup>33,49</sup> The free-standing CNM exhibits two faces, each influenced by the

## 4. Beyond SAM-based CNMs

While the fabrication of conventional CNMs starts with well-ordered SAMs, the concept can be extended. In 2013 Angelova *et al.*<sup>37</sup> tested a variety of thiol-based polyaromatic molecules as precursors, among which were ‘linear’ non-fused oligophenyl derivatives, condensed polycyclic precursors, and ‘bulky’ molecules, like the non-condensed hexaphenylbenzene derivative, and extended disc-type polycyclic aromatic hydrocarbons. Common to all these molecules was the thiol head group binding to the Au-substrate, thus still limiting the layer thickness to one monolayer. However, the near-order of the molecules in the layer strongly depends on the precursor molecules, which then affects after crosslinking properties of the CNM, like thickness, porosity, and mechanical strength.<sup>57</sup> For example, the ‘bulky’ aromatic hydrocarbons assemble to less ordered monolayers and are crosslinked into CNMs with nanometre-sized pores.<sup>37</sup> This concept can be further extended to form CNMs without the limitation of restricting the molecular layer’s thickness through selective binding of precursor mole-





cules to the substrate *via* a reactive head group. Instead, the layer thickness may be controlled by other means, for example, by the method of deposition. One option is to use slot die coating, which is an established method for casting thin organic films *e.g.* in organic light emitting diode (OLED), organic photovoltaic (OPV), or organic field effect transistor (OFET) fabrication.<sup>58</sup> Slot die coating enables precise control over the deposition of thin organic films, with layer thicknesses ranging from a few nanometres to several micrometres,<sup>59</sup> depending on the deposition conditions (movement speed of the substrate, precursor molecule flow rate and concentration, temperature). If the layer thickness is limited to one or a few molecular layers and the precursor molecules have an aromatic backbone, it is possible to crosslink such layers into a CNM by low-energy electron irradiation. This alternative method addresses limitations such as restricted micrometre lateral dimensions, expensive and sophisticated fabrication processes, and low mechanical stability. It combines the thinness of two-dimensional materials (*e.g.* few layer sheet graphene) with the chemical functionality of covalent organic frameworks (COF) and the ease of fabrication of layer-by-layer (LbL) films.<sup>37,44</sup> Again, properties of the original molecular layer as packing density or near-order of the precursor molecules are reflected in the properties of the resulting CNM.

## 5. Properties of CNMs

CNMs have a large surface-to-volume ratio, and intrinsic sub-nanometre porosity (up to 1 pore per nm<sup>2</sup> corresponding to a 40% porosity) with pores of a controlled size enabling faster passage of selected gas or liquid molecules compared to conventional filters.<sup>2,44</sup> A study conducted by Yang *et al.* revealed that CNMs made from SAMs of terphenylthiol (TPT) molecules and transferred across an 18 µm-sized aperture achieve a water permeance of  $1.13 \times 10^{-4} \text{ mol m}^{-2} \text{ s}^{-1} \text{ Pa}^{-1}$  (ref. 2) with a membrane electrical resistance of  $\sim 10^4 \Omega \text{ cm}^2$  in 1 M Cl<sup>−</sup> solution.<sup>3</sup> This suggests that water molecules pass through individual selective CNM channels at speeds similar to those in aquaporins and narrow carbon nanotubes.<sup>3</sup> Stroganov *et al.* investigated the permeation behaviour of TPT-CNM using a mass spectrometry-based setup to examine the transport of various gases, including He, Ne, D<sub>2</sub>, CO<sub>2</sub>, Ar, O<sub>2</sub>, and D<sub>2</sub>O, across a temperature range from room temperature to approximately 120 °C.<sup>60</sup> Their findings suggest that the permeation process follows a two-step mechanism: first, the gas molecules adsorb onto the nanomembrane surface, and second, they diffuse through the membrane. The study provides evidence that gas transport through ultrathin 2D materials is primarily governed by an adsorption–diffusion mechanism, which applies to a wide variety of gases and vapours.<sup>2,55</sup>

Single-layer sheets demonstrate exceptional mechanical properties, yet their breaking strength in a self-supported state diminishes with increasing lateral dimensions.<sup>61–63</sup> The CNM layer's nanometre-scale thinness makes it susceptible to defects that can arise during membrane fabrication and/or

function. When intended for use in macroscopic environments, these entities require support from porous structures, with pore sizes in the 10 nm to a few µm range contributing to enhanced stability.<sup>64</sup> Described as molecular membranes with an absence of long-range order, CNMs possess well-defined meso- and macroscopic mechanical and electrical properties, alongside distinct surface functionalities.<sup>49</sup> CNMs are unique materials that can be produced and customized to suit various environments.<sup>44,49</sup> They exhibit resilience to heat,<sup>65</sup> extended electron irradiation,<sup>56</sup> aggressive chemical conditions,<sup>42</sup> and pressure variations.<sup>41</sup> They have found applications as support materials for microscopy,<sup>40</sup> in sensors,<sup>4,5</sup> filters for both gases and liquids,<sup>49</sup> as separators in lithium metal batteries,<sup>66</sup> in biosensors,<sup>6</sup> and for applications in photocatalysis.<sup>67</sup> CNM sheets are typically insulating in the plane, but they can be made conductive through annealing at up to 900 °C, transforming them into graphene-like material.<sup>37,41,68</sup> Their thin profile, chemical surface versatility, and simple fabrication process offer high water permeance and high selectivity. These qualities make CNMs especially promising for advanced filtration and materials separation.<sup>2,44,49,60</sup>

The mechanical properties of CNMs have been studied *via* bulge tests that are frequently used to analyse the mechanical properties of free-standing films.<sup>41,57,62</sup> The technique involves the clamping of a free-standing membrane over an opening and applying pressure to one side. By analysing the pressure-deflection curves obtained, Young's modulus, tensile strength, and residual stress can be calculated.<sup>49</sup> Atomic Force Microscopy (AFM) can be utilized to assess membrane deflection either by imaging a bulged membrane using the line scanning method or by detecting the deflection of the cantilever at the membrane centre through the central point method. In the central point method, the AFM tip contacts only the membrane centre, minimizing the risk of rupture compared to full-line scanning measurements.<sup>62</sup> Both approaches have been employed to analyse the mechanical characteristics of CNMs fabricated from various molecular precursors.<sup>49,57,62,63</sup> For example, Zhang *et al.*<sup>62</sup> demonstrated that CNMs exhibit high resistance to creep deformation and remarkable tensile strength, making them ideal for applications as ultrathin support films in electron microscopy, filter membranes, and durable miniature transducers. Zhang *et al.*<sup>57</sup> found that rigid precursors like naphthalene and pyrene thiols yielded higher Young's moduli (15–19 GPa) compared to nonfused oligophenyls ( $\sim 10$  GPa), with defects and nanopores significantly affecting the mechanical properties of CNMs from less densely packed SAMs. Additionally, Dimitropoulos *et al.*<sup>63</sup> investigated the mechanical performance of CNMs made from *p*-nitrobiphenyl phosphonic acid (NBPS) and polyvinylbiphenyl (PVBp) on Si<sub>3</sub>N<sub>4</sub> substrates perforated with 0.8 µm holes, and NBPS-CNM composite membranes on track-etched polyethylene terephthalate (TE-PET). AFM and micro-tensile testing revealed that these CNMs had Young's moduli between 2.5 and 8 GPa. NBPS-CNMs exhibited higher stiffness (8 GPa) compared to PVBp-CNMs (6 GPa). This suggests that the overall mechanical performance of CNMs is influenced by the choice of precursor molecules, especially their packing



density in the molecular layer and the presence of defects. In general, small rigid precursors forming a densely packed SAM lead to higher mechanical stiffness. Overall, the mechanical characterization of transferred CNMs on supports and CNM-composite membranes demonstrated stability and resistance to degradation over long-term operation, making them suitable for various applications.<sup>63</sup>

## 6. Supports for CNMs in filtration applications

For most filtration and separation purposes, CNMs must be combined with porous support materials to ensure their mechanical strength. The selection of suitable support material plays a crucial role in determining the overall performance of CNM membranes. The density and diameter of the pores in the support material determine the ratio of the area of free-standing CNM (enabling filtration) to the total membrane area. Furthermore, the length and the shape of the support pores govern internal concentration polarization which in turn affects overall membrane mass-transfer properties.<sup>69</sup> Hence, identifying a suitable support material entails consideration of various desired characteristics to optimize membrane efficiency and effectiveness.<sup>70</sup> The support material must exhibit sufficient mechanical stability to withstand the stress and pressures experienced during membrane fabrication, handling, and operation. This ensures the longevity and reliability of the membrane under various operating conditions.<sup>71</sup> Chemical compatibility is another important consideration. The support material should be resistant to chemical degradation, particularly in environments where the membrane will be exposed to aggressive solvents.<sup>72</sup> Additionally, it should be compatible with specific applications (*e.g.* be in regulatory compliance with food processing technology<sup>73</sup>). Chemical compatibility ensures the durability and integrity of the membrane over its lifespan. Additionally, cost-effectiveness is another essential factor, especially in large-scale membrane production. The chosen support material should offer a balance between performance and affordability to ensure the economic viability of the membrane technology.<sup>72</sup> Moreover,

factors such as surface chemistry, thermal stability, and ease of fabrication and modification play significant roles in determining the suitability of support material.<sup>71</sup> Surface chemistry affects the compatibility between the support and the CNM layer, influencing the adhesion and stability of the composite membrane.<sup>63</sup>

Among potential support materials, track-etched (TE) membranes have garnered considerable interest. They have been widely adopted in diverse fields<sup>74–77</sup> and have found applications in many areas including water purification,<sup>74,78–80</sup> medical injections,<sup>81</sup> electrical neurostimulation,<sup>82</sup> and biological and biochemical sensors.<sup>83</sup> As opposed to conventional membranes, TE membranes offer distinct advantages due to their precisely determined structure.<sup>84</sup> TE membranes are produced by irradiating thin polymer films using energetic heavy ions with kinetic energies in the range of several hundred MeVs.<sup>85</sup> Within a few nanometres around the ion path, the cylindrical damage zone exhibits an increased chemical reactivity compared to the surrounding polymer matrix. These trajectories of heavy ions in a polymer membrane, known as latent tracks, are utilized for chemical etching.<sup>86</sup> Chemical etching is the pore-size and pore-shape-determining stage.<sup>84</sup> During the process, the damaged zone of a latent track is removed and transformed into a hollow channel<sup>87</sup> (Fig. 3). In the production process, two crucial parameters, pore size and pore density, stand as independently controlled parameters. Their scope ranges extensively, with pore sizes ranging from 1 nm to tens of  $\mu\text{m}$ <sup>84</sup> and pore densities varying from 1 to  $10^{10} \text{ cm}^{-2}$ .<sup>88</sup> Additionally, membrane thickness varies within the range of 5 to 50  $\mu\text{m}$  (ref. 89).

The etching process inevitably affects not only the desired tracks but also the bulk polymer. As a result, precise control over etching specificity emerges as a critical factor that exerts a profound influence on the resulting pore geometry.<sup>84,90</sup> An important parameter in etching is the etch rate, defined as the speed at which material is dissolved during etching. A precondition for the ion track formation is that the track etch rate (defined as the etch rate along the particle trajectory) is larger than the bulk etch rate (defined as the rate of dissolution of the undisturbed material outside the track).<sup>90</sup> The bulk etch rate depends on several factors, including the polymer's sensi-

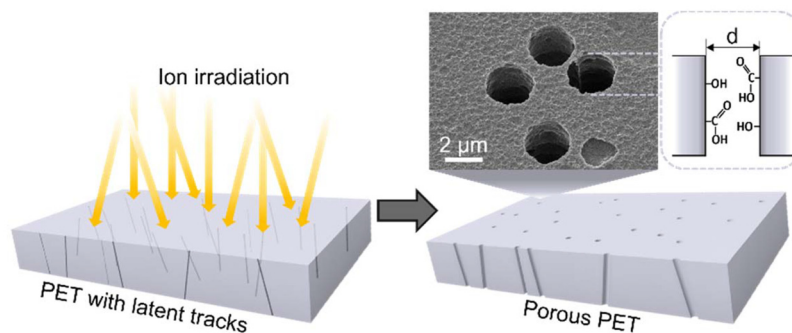


**Fig. 3** Ion track formation and chemical etching of PET to create pores. Helium ion micrograph of track-etched PET membranes with pore diameter ( $d$ ) of 2  $\mu\text{m}$  and the chemical modifications introduced during the etching process.



tivity to radiation, which is primarily determined by its molecular and supramolecular structure,<sup>90</sup> as well as irradiation conditions such as parameters of the bombarding particle, atmosphere, and temperature.<sup>84,90,91</sup> Post-irradiation treatments, such as UV exposure<sup>92–94</sup> or solvent immersion,<sup>94,95</sup> can further increase the reactivity of the latent tracks. In addition, etching parameters including the type of etchant, its temperature, and the etching time all play a crucial role in shaping the pores and determining the membrane's selectivity.<sup>84,90,96</sup> When an etching solution is applied from one side of the sample, asymmetrical pores in a conical shape can be produced.<sup>97</sup> The criteria for a suitable material for track-etching include chemical and mechanical stability to maintain robustness as an eventual membrane, availability as a thin film, sensitivity towards ion irradiation and chemically selective etching of ion tracks.<sup>90,98</sup> Among the various polymers evaluated, three have emerged as dominant: polycarbonate (PC),<sup>80,99–102</sup> polyimide (PI),<sup>84,103,104</sup> and polyethylene terephthalate (PET).<sup>76,79,105,106</sup> Of these, PET stands out as a highly stable polymer with high resistance to acids, organic solvents, and biological degradation. It is renowned for its robust mechanical strength, making it suitable for a wide array of applications.<sup>84,107</sup> One key advantage of PET is its high etch rate ratio, allowing it to produce membranes with tunable pore diameters by adjusting etching conditions such as time, temperature, and solution concentration, involving the use of alkali solutions to develop tracks.<sup>84</sup>

Several studies have examined TE-PET membranes with targeted modifications and applications, such as increasing surface hydrophobicity to enable membrane distillation<sup>107</sup> and oil–water separation,<sup>74</sup> as well as using TE-PET for desalination.<sup>108</sup> Additionally, TE-PET membranes have been investigated for gas separation,<sup>109</sup> as separators in lithium batteries<sup>110,111</sup> and in pharmaceutical separation processes.<sup>112</sup> In a study by Yang *et al.*, double-layer CNMs were transferred onto a track-etched PET support and tested in forward osmosis (FO) filtration. Water permeance of  $2 \times 10^{-6} \text{ mol m}^{-2} \text{ s}^{-1} \text{ Pa}^{-1}$  was measured,<sup>3</sup> which is lower than the reported value of  $1.13 \times 10^{-4} \text{ mol m}^{-2} \text{ s}^{-1} \text{ Pa}^{-1}$  from mass-loss measurements,<sup>2</sup> likely due to the effects of internal and external concentration polarization, phenomena that occur when solute concentration changes at the membrane surface (external) or within the membrane support layer (internal) compared to the respective concentrations in the solutions in the volume. Concentration polarization can lead to a reduced effective osmotic gradient, affecting water permeance.<sup>113</sup> Additionally, the two studies differ in their driving forces: in mass loss measurements, pervaporation is driven by a vapor pressure gradient, where the partial pressure difference between the interior and exterior of the container, on which the CNM is mounted, drives the separation process. In contrast, in FO, the osmotic pressure difference between the feed solution and the draw solution facilitates the movement of water across a semi-permeable membrane. The driving forces must be carefully considered when evaluating and comparing the performance of these processes. In addition, the study reported a reverse salt flux of  $0.1 \text{ g L}^{-1}$

which is the ratio of reverse salt mass flux to forward water flux in FO filtration.<sup>3</sup> In an ideal semipermeable membrane, reverse salt flux would be zero, meaning no salt would pass through the membrane in the reverse direction. Most commercially available FO membranes typically report values of  $0.2 \text{ g L}^{-1}$  or higher.<sup>114</sup> The reverse salt flux can influence the performance of the membrane, potentially reducing the efficiency of the filtration process.<sup>115</sup> These results were confirmed through concentration-gradient-driven diffusion experiments conducted in both neutral and acidic conditions.<sup>116</sup> Moreover, the study revealed that water transport through the double-layered structure is similar to that of through a single CNM layer, which can be explained by the single-file transport mechanism, where the flow rate remains unaffected by the length of the channel.<sup>3,117</sup> When CNM layers are stacked atop one another, they are bound together by van der Waals forces, creating interlayer spaces between the layers. When stacking multiple CNM layers, it is unlikely that the channels in each layer align perfectly. Instead, the channels are typically offset from one another in different layers, creating a more complex network for transport.<sup>118</sup> The single-file path begins by passing through a channel in the first CNM layer, then continues through the confined space between the two layers and finally exits through a channel in the second CNM layer. While the transport of pure water seems unaffected by the double layer of CNMs, transport is hindered for organic molecules.<sup>119</sup> A phenomenon known as ‘molecular jam’ occurs within the nanochannels, where the accumulation of organic molecules creates a diffusion barrier. This barrier increases the concentration of these molecules between the layers, disrupting the orderly single-file movement of water molecules and hindering their flow.<sup>119</sup>

One observed property of TE-PET-support in long term filtration is the gradual decline in water permeability due to swelling.<sup>90,120</sup> The pristine PET has a water contact angle of approximately  $72^\circ$ .<sup>121</sup> However, after the etching process, the surface becomes more hydrophilic. This transformation is attributed to the formation of a few nanometres thin surface layer containing a much higher concentration of carboxyl ( $-\text{COOH}$ ) and hydroxyl ( $-\text{OH}$ ) end groups than in the untreated polymer.<sup>90</sup> This hydrophilized surface can take up water and swell in volume, thus reducing the radius of the track-etched pores over time. According to the Hagen–Poiseuille equation, applicable to membranes with an array of uniform cylindrical pores, membrane permeability is proportional to the square of the pore radius and the pore density. Therefore, even a slight reduction in pore radius due to swelling can lead to a significant flux decrease.<sup>90,121,122</sup> It was observed that the swelling of the TE-PET support has a smaller impact in FO systems compared to pressure-driven processes. Moreover, in pressure-driven processes, micron-sized defects in the CNM-layer heavily affect the water flux (orders of magnitude higher than through intact CNM-layers). Additionally, this free flux through these defects comprises minimal or no solute rejection, thus significantly affecting the overall membrane performance. In FO systems, however, where water transport is driven by



osmotic pressure, these defects tend to have a less pronounced effect on overall performance.<sup>69</sup> This impact suggests that TE-PET-supported CNM membranes could be more suitable for osmosis-driven applications, while pressure-driven processes may still require further to improve overall performance. Overall, these studies underscore the critical importance of considering support material properties in membrane design and optimization, illuminating a fundamental aspect of composite membrane behaviour.

## 7. Large-area CNM-composite membranes

Despite the challenge of swelling, TE-PET remains highly promising support for a CNM in filtration applications. However, the conventional transfer step presents challenges that may lead to ruptures or defects of the ultrathin CNM, ultimately reducing overall performance.<sup>123,124</sup> As a result, the use

of transferred CNMs seems more favourable for applications that do not require a large active area per device, such as sensors and drug delivery systems. To address the risk of handling-related damage, the concept of CNM-composite membranes is proposed, where the CNM layer is fabricated directly on the porous support and the need for a transfer step is eliminated (Fig. 4).<sup>50,123</sup>

The concept of CNM-composite membranes begins with ion-beamed PET as the growth substrate for the CNM. Its continuous surface presents an opportunity to create a pinhole-free, molecular-thin film of aromatic precursor molecules on one side. Upon exposure to low-energy electrons, precursor molecules are crosslinked, forming a chemically and thermally stable CNM (Fig. 5).

The stability of the CNM layer extends to withstanding the alkaline etching of the latent pores within the PET matrix. The characteristics of the CNM active layer, particularly its thickness and intrinsic porosity, rely on the selection of precursor molecules and the conditions during preparation.<sup>44</sup> Since it is

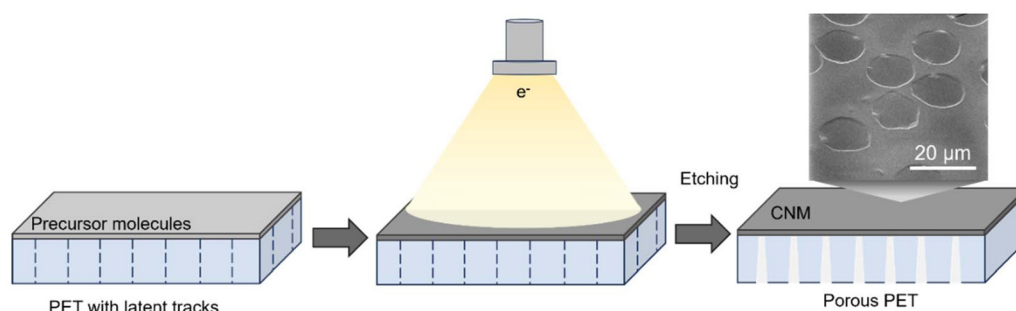


**Fig. 4** Three-step manufacturing process of a CNM-composite membrane: (i) deposition of precursor molecules on beamed PET with latent pores, (ii) electron-induced crosslinking, and (iii) one-sided etching. The helium ion micrograph shows the surface of the final CNM-composite membrane.

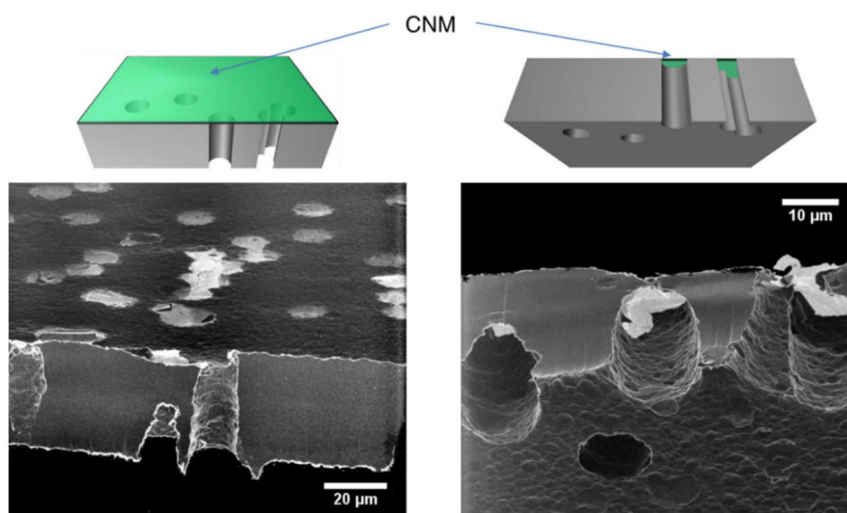


**Fig. 5** Helium ion micrograph of a cross-section of a CNM-composite membrane. The free-standing CNM the active layer of the composite membrane, (depicted in green in the sketch on the top) can be identified as the bright areas.





not possible to form a well-ordered SAM on the PET surface, it has not been possible up to now to form a CNM-layer with the exceptional properties of TPT-CNMs,<sup>2</sup> in comparison to other commercially available FO membranes.<sup>125</sup> However, various types of beyond-SAM-based CNMs with their advantage of scalable production have been and are investigated as potential active layers in CNM-composite membranes for hydraulic pressure-driven and osmosis-driven separation processes with promising results (e.g. CNM-layer with reverse salt flux of 0.9 g L<sup>-1</sup> in FO with draw solution of 1 M NaCl, achieved with a CNM layer of just crosslinked aromatic PET polymer molecules<sup>123</sup>). Such performance can only be achieved in FO filtration with defect rates of CNM-layer of less than 1%<sup>69</sup> one effective approach to further mitigate these defects, which may arise during fabrication, handling, or testing of the CNM layer, is through the application of interfacial polymerization. This approach effectively heals defects with a polymer layer reducing the free water flux through the defects while maintaining the sub-nanometre pores within the CNMs.<sup>124</sup>

## 8. Conclusion

Self-assembly has evolved from early studies of molecular monolayers by Langmuir and Blodgett to advanced applications in nanotechnology, with the transition from SAMs to CNMs highlighting a significant advancement in material science. The choice of precursor molecules and the conditions during their preparation influence the properties of CNMs, including their thickness, porosity, and mechanical strength. Applications of CNMs vary from filtration technologies to electronic devices, benefiting from their thin profile, high chemical stability, and customizable surface functionalities. However, for some practical applications such as filtration, CNMs require support materials to ensure their mechanical stability. The challenges of support material properties and the risk of membrane damage during the transfer procedure highlight the need for continued innovation in membrane fabrication. Despite some challenges, such as swelling, TE-PET is a promising support material because CNMs can be directly formed on its surface before the latent pores in the PET layer are opened through chemical etching. Overall, CNMs present a promising frontier in material science, offering exceptional characteristics such as molecular-scale thickness, high permeability, tunable surface functionality, and robust mechanical and chemical stability, which make them highly promising for advanced filtration technologies and nanoscale device integration.

## Conflicts of interest

A. S. and A. G. are the co-founders of CNM Technologies GmbH, a company focused on developing and marketing CNMs and CNM-composite membranes. A. S. is also CEO of the company and is listed as an inventor on the international

patent application WO 2019/228956 A1, titled “Carbon Nanomembranes on Porous Materials” as well as U.S. Patent US 10.646.831 B2 titled “Method for manufacturing of a carbon nanomembrane” (both assigned to CNM Technologies GmbH), which covers the manufacturing process of CNM-composite membranes. A. G. is listed as an inventor on the international patent application US 8.377.243 B2 titled “Method for transferring a nanolayer” and US 9.186.630 B2 titled “Perforated Membranes”. The other authors declare no conflicts of interest.

## Data availability

This review does not include any primary research data, software, or code, nor were any new data generated or analyzed in the course of this work. A limited portion of unpublished data, which is in preparation for publication, has been referenced, with results briefly discussed.

## References

- 1 Z. Yao, N. Meyerbröcker, Y. Qi, J. Cremer, M. Westphal, D. Anselmetti, Y. Yang and A. Götzhäuser, *ACS Appl. Mater. Interfaces*, 2023, **15**, 41101–41108.
- 2 Y. Yang, P. Dementyev, N. Biere, D. Emmrich, P. Stohmann, R. Korzetz, X. Zhang, A. Beyer, S. Koch, D. Anselmetti and A. Götzhäuser, *ACS Nano*, 2018, **12**, 4695–4701.
- 3 Y. Yang, R. Hillmann, Y. Qi, R. Korzetz, N. Biere, D. Emmrich, M. Westphal, B. Büker, A. Hütten, A. Beyer, D. Anselmetti and A. Götzhäuser, *Adv. Mater.*, 2020, **32**, 1907850.
- 4 X. Zhang, R. Waitz, F. Yang, C. Lutz, P. Angelova, A. Götzhäuser and E. Scheer, *Appl. Phys. Lett.*, 2015, **106**, 063107.
- 5 D. Kaiser, Z. Tang, M. Küllmer, C. Neumann, A. Winter, R. Kahle, L. Georgi, T. Weimann, M. Siegmann, S. Gräfe, A. Centeno, A. Zurutuza and A. Turchanin, *Appl. Phys. Rev.*, 2021, **8**, 031410.
- 6 D. Kaiser, N. Meyerbroeker, W. Purschke, S. Sell, C. Neumann, A. Winter, Z. Tang, D. Hüger, C. Maasch, L. Bethge, T. Weimann, G. Ferwerda, M. I. de Jonge, A. Schnieders, A. Vater and A. Turchanin, *Adv. Mater.*, 2024, **36**, 2407487.
- 7 B. R. Hughes and Y. Dahman, in *Fabrication and Self-Assembly of Nanobiomaterials*, ed. A. M. Grumezescu, William Andrew Publishing, 2016.
- 8 G. A. Ozin, K. Hou, B. V. Lotsch, L. Cademartiri, D. P. Puzzo, F. Scotognella, A. Ghadimi and J. Thomson, *Mater. Today*, 2009, **12**, 12–23.
- 9 A. Ulman, *Chem. Rev.*, 1996, **96**, 1533–1554.
- 10 J. C. Love, L. A. Estroff, J. K. Kriebel, R. G. Nuzzo and G. M. Whitesides, *Chem. Rev.*, 2005, **105**, 1103–1170.
- 11 S. Casalini, C. A. Bortolotti, F. Leonardi and F. Biscarini, *Chem. Soc. Rev.*, 2017, **46**, 40–71.



- 12 S. A. Claridge, W.-S. Liao, J. C. Thomas, Y. Zhao, H. H. Cao, S. Cheunkar, A. C. Serino, A. M. Andrews and P. S. Weiss, *Chem. Soc. Rev.*, 2013, **42**, 2725–2745.
- 13 E. Ruckenstein and Z. F. Li, *Adv. Colloid Interface Sci.*, 2005, **113**, 43–63.
- 14 C. Nicosia and J. Huskens, *Mater. Horiz.*, 2014, **1**, 32–45.
- 15 R. Ruvalcaba, Z. Liu, M. I. Nugraha, G. Harrison, Y.-Y. Yang, M. Thaler, A. V. Marsh, M. Zeilerbauer, C. Aivalioti, R. R. Aguilera-Vazquez, L. Tsetseris, L. L. Patera, P. Zahl, M. Heeney, T. D. Anthopoulos and S. Fatayer, *ACS Mater. Lett.*, 2025, **7**, 1421–1430.
- 16 P. Cyganik, A. Terfort and M. Zharnikov, *Nano Res.*, 2024, **17**, 4231–4243.
- 17 G. Roberts, *Langmuir-Blodgett Films*, Springer, New York, 1990.
- 18 A. Ulman, *An introduction to ultrathin organic films: From Langmuir-Blodgett to self-assembly*, Academic Press, San Diego, 1991.
- 19 M. C. Petty, *Langmuir-Blodgett Films*, 1996.
- 20 W. C. Bigelow, *et al.*, *J. Coll. Sci.*, 1946, **1**, 513.
- 21 J. Sagiv, *J. Am. Chem. Soc.*, 1980, **102**, 92–98.
- 22 E. E. Polymeropoulos and J. Sagiv, *J. Chem. Phys.*, 1978, **69**, 1836–1847.
- 23 R. G. Nuzzo and D. L. Allara, *J. Am. Chem. Soc.*, 1983, **105**, 4481–4483.
- 24 G. K. Jennings and P. E. Laibinis, *J. Am. Chem. Soc.*, 1997, **119**, 5208–5214.
- 25 P. E. Laibinis, G. M. Whitesides, D. L. Allara, Y. T. Tao, A. N. Parikh and R. G. Nuzzo, *J. Am. Chem. Soc.*, 1991, **113**, 7152–7167.
- 26 C. Vericat, M. E. Vela, G. Corthey, E. Pensa, E. Cortés, M. H. Fonticelli, F. Ibañez, G. E. Benitez, P. Carro and R. C. Salvarezza, *RSC Adv.*, 2014, **4**, 27730–27754.
- 27 M. M. Walczak, C. Chung, S. M. Stole, C. A. Widrig and M. D. Porter, *J. Am. Chem. Soc.*, 1991, **113**, 2370–2378.
- 28 W. Zhao, M. Göthelid, S. Hosseinpour, M. B. Johansson, G. Li, C. Leygraf and C. M. Johnson, *J. Colloid Interface Sci.*, 2021, **581**, 816–825.
- 29 Z. Duan, Z. Xie, Y. Hu, J. Xu, J. Ren, Y. Liu and H.-Y. Nie, *Molecules*, 2024, **29**, 706.
- 30 M. Dubey, T. Weidner, L. J. Gamble and D. G. Castner, *Langmuir*, 2010, **26**, 14747–14754.
- 31 M. Wang, K. M. Liechti, Q. Wang and J. M. White, *Langmuir*, 2005, **21**, 1848–1857.
- 32 L. Wang, U. S. Schubert and S. Hoeppeener, *Chem. Soc. Rev.*, 2021, **50**, 6507–6540.
- 33 C. Neumann, M. Szwed, M. Frey, Z. Tang, K. Koziel, P. Cyganik and A. Turchanin, *ACS Appl. Mater. Interfaces*, 2019, **11**, 31176–31181.
- 34 A. Asyuda, R. O. de la Morena, E. Sauter, K. Turner, K. McDonald, M. Buck and M. Zharnikov, *J. Phys. Chem. C*, 2020, **124**, 25107–25120.
- 35 M. Kruk, C. Neumann, M. Frey, K. Koziel, A. Turchanin and P. Cyganik, *J. Phys. Chem. C*, 2021, **125**, 9310–9318.
- 36 P. Dementyev, D. Naberezhnyi, M. Westphal, M. Buck and A. Götzhäuser, *ChemPhysChem*, 2020, **21**, 1006–1011.
- 37 P. Angelova, H. Vieker, N.-E. Weber, D. Matei, O. Reimer, I. Meier, S. Kurasch, J. Biskupek, D. Lorbach, K. Wunderlich, L. Chen, A. Terfort, M. Klapper, K. Müllen, U. Kaiser, A. Götzhäuser and A. Turchanin, *ACS Nano*, 2013, **7**, 6489–6497.
- 38 C. Preischl, L. H. Le, E. Bilgilişoy, A. Götzhäuser and H. Marbach, *Beilstein J. Nanotechnol.*, 2021, **12**, 319–329.
- 39 A. Turchanin and A. Götzhäuser, *Prog. Surf. Sci.*, 2012, **87**, 108–162.
- 40 C. T. Nottbohm, A. Beyer, A. S. Sologubenko, I. Ennen, A. Hütten, H. Rösner, W. Eck, J. Mayer and A. Götzhäuser, *Ultramicroscopy*, 2008, **108**, 885–892.
- 41 A. Turchanin, A. Beyer, C. T. Nottbohm, X. Zhang, R. Stosch, A. Sologubenko, J. Mayer, P. Hinze, T. Weimann and A. Götzhäuser, *Adv. Mater.*, 2009, **21**, 1233–1237.
- 42 W. Eck, A. Küller, M. Grunze, B. Völkel and A. Götzhäuser, *Adv. Mater.*, 2005, **17**, 2583–2587.
- 43 A. Götzhäuser, C. Nottbohm and A. Beyer, Method for transferring a nanolayer, US 8.377.243B2, 2013.
- 44 P. Angelova and A. Götzhäuser, in *Chemistry of Carbon Nanostructures*, ed. K. Muellen and F. Xinliang, De Gruyter, 2017.
- 45 D. M. Cegiela, M. Frey, K. Koziel, C. Neumann, A. Turchanin and P. Cyganik, *J. Phys. Chem. Lett.*, 2024, **15**, 8196–8204.
- 46 C. M. Crudden, J. H. Horton, I. I. Ebralidze, O. V. Zenkina, A. B. McLean, B. Drevniok, Z. She, H.-B. Kraatz, N. J. Mosey, T. Seki, E. C. Keske, J. D. Leake, A. Rousina-Webb and G. Wu, *Nat. Chem.*, 2014, **6**, 409–414.
- 47 C. M. Crudden, J. H. Horton, M. R. Narouz, Z. Li, C. A. Smith, K. Munro, C. J. Baddeley, C. R. Larrea, B. Drevniok, B. Thanabalasingam, A. B. McLean, O. V. Zenkina, I. I. Ebralidze, Z. She, H.-B. Kraatz, N. J. Mosey, L. N. Saunders and A. Yagi, *Nat. Commun.*, 2016, **7**, 12654.
- 48 N. L. Dominique, A. Chandran, I. M. Jensen, D. M. Jenkins and J. P. Camden, *Chem. – Eur. J.*, 2024, **30**, e202303681.
- 49 A. Turchanin and A. Götzhäuser, *Adv. Mater.*, 2016, **28**, 6075–6103.
- 50 P. Angelova and A. Schnieders, Method for manufacturing of a carbon nanomembrane, US 10.646.831B2, 2020.
- 51 C. Neumann, R. A. Wilhelm, M. Küllmer and A. Turchanin, *Faraday Discuss.*, 2021, **227**, 61–79.
- 52 A. Götzhäuser, W. Geyer, V. Stadler, W. Eck, M. Grunze, K. Edinger, T. Weimann and P. Hinze, *J. Vac. Sci. Technol., B: Microelectron. Nanometer Struct.–Process., Meas., Phenom.*, 2000, **18**, 3414–3418.
- 53 G. Kaltenpoth, B. Völkel, C. T. Nottbohm, A. Götzhäuser and M. Buck, *J. Vac. Sci. Technol., B: Microelectron. Nanometer Struct.–Process., Meas., Phenom.*, 2002, **20**, 2734–2738.
- 54 A. Turchanin, A. Tinazli, M. El-Desawy, H. Großmann, M. Schnietz, H. H. Solak, R. Tampé and A. Götzhäuser, *Adv. Mater.*, 2008, **20**, 471–477.



- 55 V. Stroganov, T. Nöthel, D. Hüger, M. Kruk, C. Neumann, K. Koziel, P. Cyganik and A. Turchanin, *Small*, 2024, **20**, 2406526.
- 56 A. Turchanin, D. Käfer, M. El-Desawy, C. Wöll, G. Witte and A. Götzhäuser, *Langmuir*, 2009, **25**, 7342–7352.
- 57 X. Zhang, C. Neumann, P. Angelova, A. Beyer and A. Götzhäuser, *Langmuir*, 2014, **30**, 8221–8227.
- 58 X. Ding, J. Liu and T. A. L. Harris, *AIChE J.*, 2016, **62**, 2508–2524.
- 59 R. Keshavarzi, F. Hajisharifi, Z. Saki, M. Omrani, R. Sheibani, N. Afzali, M. Abdi-Jalebi, L. Vesce and A. Di Carlo, *Nano Today*, 2025, **61**, 102600.
- 60 V. Stroganov, D. Hüger, C. Neumann, T. Noethel, M. Steinert, U. Hübner and A. Turchanin, *Small*, 2023, **19**, 2300282.
- 61 D. Cohen-Tanugi and J. C. Grossman, *Nano Lett.*, 2014, **14**, 6171–6178.
- 62 X. Zhang, A. Beyer and A. Götzhäuser, *Beilstein J. Nanotechnol.*, 2011, **2**, 826–833.
- 63 M. Dimitropoulos, G. Trakakis, N. Meyerbröcker, R. Gehra, P. Angelova, A. Schnieders, C. Pavlou, C. Kostaras, C. Galiotis and K. Dassios, *Nanomaterials*, 2023, **13**, 267.
- 64 L. Wang, C. M. Williams, M. S. H. Boutilier, P. R. Kidambi and R. Karnik, *Nano Lett.*, 2017, **17**, 3081–3088.
- 65 A. Turchanin, M. El-Desawy and A. Götzhäuser, *Appl. Phys. Lett.*, 2007, **90**, 053102.
- 66 S. Rajendran, Z. Tang, A. George, A. Cannon, C. Neumann, A. Sawas, E. Ryan, A. Turchanin and L. M. R. Arava, *Adv. Energy Mater.*, 2021, **11**, 2100666.
- 67 M. Küllmer, F. Herrmann-Westendorf, P. Endres, S. Götz, H. Reza Rasouli, E. Najafidehaghani, C. Neumann, R. Gläßner, D. Kaiser, T. Weimann, A. Winter, U. S. Schubert, B. Dietzek-Ivanšić and A. Turchanin, *Angew. Chem., Int. Ed.*, 2022, **61**, e202204953.
- 68 D. G. Matei, N.-E. Weber, S. Kurasch, S. Wundrack, M. Woszczyzna, M. Grothe, T. Weimann, F. Ahlers, R. Stosch, U. Kaiser and A. Turchanin, *Adv. Mater.*, 2013, **25**, 4146–4151.
- 69 M. Giagnorio, B. Tanis, C. Hélix-Nielsen and F. J. Aschmoneit, *Sep. Purif. Technol.*, 2024, **330**, 125182.
- 70 E. Drioli and L. Giorno, *Encyclopedia of Membranes*, Springer, 2019.
- 71 H. Mokarizadeh, S. Moayedfard, M. S. Maleh, S. I. G. P. Mohamed, S. Nejati and M. R. Esfahani, *Sep. Purif. Technol.*, 2021, **278**, 119451.
- 72 W. J. Lau, A. F. Ismail, N. Misdan and M. A. Kassim, *Desalination*, 2012, **287**, 190–199.
- 73 S. Priyanka, S. Karthick Raja Namasivayam and R. S. Arvind Bharani, *Chemosphere*, 2023, **336**, 139240.
- 74 I. V. Korolkov, A. R. Narmukhamedova, G. B. Melnikova, I. B. Muslimova, A. B. Yeszhanov, Z. K. Zhatkanbayeva, S. A. Chizhik and M. V. Zdorovets, *Membranes*, 2021, **11**, 637.
- 75 I. V. Korolkov, A. B. Yeszhanov, M. V. Zdorovets, Y. G. Gorin, O. Güven, S. S. Dosmagambetova, N. A. Khlebnikov, K. V. Serkov, M. V. Krasnopyorova, O. S. Milts and D. A. Zheltov, *Sep. Purif. Technol.*, 2019, **227**, 115694.
- 76 K. Daumann, S. Frost and M. Ulbricht, *RSC Adv.*, 2020, **10**, 21028–21038.
- 77 M. V. Zdorovets, A. B. Yeszhanov, I. V. Korolkov, O. Güven, S. S. Dosmagambetova, D. I. Shlimas, Z. K. Zhatkanbayeva, I. S. Zhidkov, P. V. Kharkin, V. N. Gluchshenko, D. A. Zheltov, N. A. Khlebnikov and I. E. Kuklin, *Prog. Nucl. Energy*, 2020, **118**, 103128.
- 78 I. V. Korolkov, A. B. Yeszhanov, Y. G. Gorin, M. V. Zdorovets, N. A. Khlebnikov and K. V. Serkov, *Mater. Res. Express*, 2018, **5**, 065317.
- 79 A. A. Belkova, A. I. Sergeeva, P. Y. Apel and M. K. Beklemishev, *J. Membr. Sci.*, 2009, **330**, 145–155.
- 80 A. Popova, S. Boivin, T. Shintani and T. Fujioka, *Desalination*, 2024, **572**, 117155.
- 81 Z.-B. He and S. L. Guo, *Phys. Procedia*, 2015, **80**, 131–134.
- 82 V. Trofimov, D. Kukushkin, A. Vasilev, I. Arhipushkin, V. Kublanov, M. Babich, A. Dolganov and V. Gadelshin, *Application of track membranes in electrodes for electrical neurostimulation*, 2015.
- 83 H. Hanot, *Am. Biotechnol. Lab.*, 2007, **25**, 24–26.
- 84 P. Y. Apel, *Radiat. Meas.*, 2001, **34**, 559–566.
- 85 S. Kumar, S. Kumar and S. K. Chakarvarti, *Radiat. Meas.*, 2003, **36**, 757–760.
- 86 D. Chander, R. Kumar, S. Kumar, D. Kumar and P. Chakarvarti, *Nano*, 2018, **13**, 012050.
- 87 R. L. Fleischer, P. B. Price, R. M. Walker and R. M. Walker, *Nuclear Tracks in Solids: Principles and Applications*, University of California Press, 1975.
- 88 B. S. Lalia, V. Kochkodan, R. Hashaikeh and N. Hilal, *Desalination*, 2013, **326**, 77–95.
- 89 S. Makkonen-Craig, K. Yashina and M. Paronen, *Chem. Sci.*, 2014, **116**, 1–13.
- 90 D. Fink, *Fundamentals of ion-irradiated polymers*, Springer Science & Business Media, 2004.
- 91 P. Y. Apel, A. Y. Didyk, B. I. Fursov, L. I. Kravets, V. G. Nesterov, L. I. Samoilova and G. S. Zhdanov, *Radiat. Meas.*, 1997, **28**, 19–24.
- 92 Z. Zhu, Y. Maekawa, Q. Liu and M. Yoshida, *Nucl. Instrum. Methods Phys. Res., Sect. B*, 2005, **236**, 61–67.
- 93 P. Y. Apel, I. V. Blonskaya, N. E. Lizunov, K. Olejniczak, O. L. Orellovitch, M. E. Toimil-Molares and C. Trautmann, *Small*, 2018, **14**, 1703327.
- 94 Z. Zhu, Y. Maekawa, H. Koshikawa, Y. Suzuki, N. Yonezawa and M. Yoshida, *Nucl. Instrum. Methods Phys. Res., Sect. B*, 2004, **217**, 449–456.
- 95 P. Y. Apel, N. Angert, W. Bruchle, H. Hermann, U. Kampschulte, P. Klein, L. I. Kravets, Y. T. Oganessian, G. Remmert, R. Spohr, T. Steckenreiter, C. Trautmann and J. Vetter, *Nucl. Instrum. Methods Phys. Res., Sect. B*, 1994, **86**, 325–332.
- 96 P. Y. Apel and S. N. Dmitriev, *Adv. Nat. Sci.: Nanosci. Nanotechnol.*, 2011, **2**, 013002.
- 97 P. Y. Apel, V. V. Bashevov, I. V. Blonskaya, N. E. Lizunov, O. L. Orellovitch and C. Trautmann, *Phys. Chem. Chem. Phys.*, 2016, **18**, 25421–25433.



- 98 R. Spohr and K. Bethge, *Ion Tracks and Microtechnology: Principles and Applications*, Vieweg+Teubner Verlag, 1990.
- 99 K.-J. Hwang and Y.-C. Chiang, *Sep. Purif. Technol.*, 2014, **125**, 74–82.
- 100 L. Zhu, W. Jia, M. Kattula, K. Ponnuru, E. P. Furlani and H. Lin, *J. Membr. Sci.*, 2016, **514**, 684–695.
- 101 S. Dutt, P. Y. Apel, N. Lizunov, C. Notthoff, Q. Wen, C. Trautmann, P. Mota-Santiago, N. Kirby and P. Kluth, *J. Membr. Sci.*, 2021, **638**, 119681.
- 102 T. W. Cornelius, P. Y. Apel, B. Schiedt, C. Trautmann, M. E. Toimil-Molares, S. Karim and R. Neumann, *Nucl. Instrum. Methods Phys. Res., Sect. B*, 2007, **265**, 553–557.
- 103 P. Y. Apel, I. V. Blonskaya, V. R. Oganessian, O. L. Orellovitch and C. Trautmann, *Nucl. Instrum. Methods Phys. Res., Sect. B*, 2001, **185**, 216–221.
- 104 K. Froehlich, M. C. Scheuerlein, M. Ali, S. Nasir and W. Ensinger, *Nanotechnology*, 2022, **33**, 045301.
- 105 I. V. Korolkov, O. Güven, A. A. Mashentseva, A. B. Atıcı, Y. G. Gorin, M. V. Zdorovets and A. A. Taltenov, *Radiat. Phys. Chem.*, 2017, **130**, 480–487.
- 106 I. V. Korolkov, A. A. Mashentseva, O. Güven, Y. G. Gorin and M. V. Zdorovets, *Radiat. Phys. Chem.*, 2018, **151**, 141–148.
- 107 I. V. Korolkov, A. A. Mashentseva, O. Güven, M. V. Zdorovets and A. A. Taltenov, *Nucl. Instrum. Methods Phys. Res., Sect. B*, 2015, **365**, 651–655.
- 108 V. Satulu, B. Mitu, V. A. Altynov, N. E. Lizunov, L. Kravets and G. Dinescu, *Thin Solid Films*, 2017, **630**, 92–99.
- 109 S. Takahashi, M. Yoshida, M. Asano and T. Nakagawa, *Polym. J.*, 2004, **36**, 50–53.
- 110 P. L. J. Lee, V. Thangavel, C. Guery, C. Trautmann, M. E. Toimil-Molares and M. Morcrette, *Nanotechnology*, 2021, **32**, 365401.
- 111 J. Liu, D. Cao, H. Yao, D. Liu, X. Zhang, Q. Zhang, L. Chen, S. Wu, Y. Sun, D. He and J. Liu, *ACS Appl. Energy Mater.*, 2022, **5**, 8639–8649.
- 112 K. Cuanalo-Contreras, A. M. R. Hogrebe, K. Teichmann and D. Benkmann, *Chem. Ing. Tech.*, 2023, **95**, 1372–1380.
- 113 J. R. McCutcheon and M. Elimelech, *J. Membr. Sci.*, 2006, **284**, 237–247.
- 114 M. Tian, T. Ma, K. Goh, Z. Pei, J. Y. Chong and Y.-N. Wang, *Membr.*, 2022, **12**, 955.
- 115 S. Zou, M. Qin and Z. He, *Water Res.*, 2019, **149**, 362–374.
- 116 R. Dalpke, A. Dreyer, R. Korzetz, K.-J. Dietz and A. Beyer, *J. Phys. Chem. Lett.*, 2020, **11**, 6737–6741.
- 117 A. Kalra, S. Garde and G. Hummer, *Proc. Natl. Acad. Sci. U. S. A.*, 2003, **100**, 10175–10180.
- 118 M. Ai, S. Shishatskiy, J. Wind, X. Zhang, C. T. Nottbohm, N. Mellech, A. Winter, H. Vieker, J. Qiu, K.-J. Dietz, A. Götzhäuser and A. Beyer, *Adv. Mater.*, 2014, **26**, 3421–3426.
- 119 P. Dementyev, Y. Yang, M. Rezvova and A. Götzhäuser, *J. Phys. Chem. Lett.*, 2020, **11**, 238–242.
- 120 P. Y. Apel, Y. E. Korchev, Z. Siwy, R. Spohr and M. Yoshida, *Nucl. Instrum. Methods Phys. Res., Sect. B*, 2001, **184**, 337–346.
- 121 D. Fink, S. Ghosh, R. Klett, K. K. Dwivedi, Y. Kobayashi, K. Hirata, J. Vacik, V. Hnatowicz, J. Cervena and L. T. Chadderton, *Nucl. Instrum. Methods Phys. Res., Sect. B*, 1998, **146**, 486–490.
- 122 D. M. Kanani, W. H. Fissell, S. Roy, A. Dubnisheva, A. Fleischman and A. L. Zydney, *J. Membr. Sci.*, 2010, **349**, 405–410.
- 123 N. Meyerbröcker, P. Angelova, A. Schnieders and H. Vieker, Carbon nanomembranes on porous materials, US 11.666.866B2, 2023.
- 124 Z. Yao, P. Li, K. Chen, Y. Yang, A. Beyer, M. Westphal, Q. J. Niu and A. Götzhäuser, *ACS Appl. Mater. Interfaces*, 2024, **16**, 22614–22621.
- 125 W. Suwaileh, N. Pathak, H. Shon and N. Hilal, *Desalination*, 2020, **485**, 114455.

